48th AIAA/ASME/ASCE/AHS/ASC Structures, Structural Dynamics, and Materials Conference
23 - 26 April 2007, Honolulu, Hawaii

AIAA 2007-1837

Synchronous Deployed Solar Sail Subsystem Design Concept

Jeremy A. Banik[1]
CSA Engineering, Inc., Albuquerque, New Mexico, 87123

and
Thomas W. Murphey[2]
Air Force Research Laboratory, Albuquerque, New Mexico, 87117

A solar sail concept has been developed from a common spiral fold pattern in order to enable a simultaneous mast and sail deployment. This novel concept utilizes the stored strain energy in a series of elastic spar members to enforce proper folding kinematics rather than relying on bulky mechanical joints. The critical inner and outer spar networks are secured to four elastically extendible masts anchored to a central drum. Deployment of the solar sail system is actuated by rotating the central drum around which the masts, spars, and film are wrapped. Tensioned radial cords deterministically unfold the membrane film under the authority of the resilient, spring-like spar members. Proper elastic behavior of the spars is an important facet to this design, and thus a significant effort was dedicated their development. This compact ground demonstration concept includes about 7.5 m^2 of reflective membrane film for useful propulsion. Features of this robust, lightweight membrane structure may prove valuable to reducing mass and increasing deployment reliability of other planar subsystems such as sun shades, solar arrays, radiators, or antenna arrays.

Nomenclature

L	=	Side length of polygonal drum
R	=	Drum radius
h	=	Wrapped height
n	=	Number of gores
s	=	Characteristic length of one sail side
w	=	Peak fold shifted distance
α	=	Interior angle of polygonal drum

I. Introduction

NEARLY every modern spacecraft has a subsystem that requires some degree of deployable functionality, whether the subsystem be an antenna, a solar array, a radiator, a sun shade, or a solar sail. As the spacecraft community continues to call upon large deployable subsystems to fulfill new mission requirements, new deployable architectures must be developed to meet these new functional needs as well as to reduce mass, increase packaging efficiency, and increase deployment reliability. The synchronous deployed solar sail concept presented here demonstrates a simple method to simultaneously deploy both masts and membrane film in a deterministic way for an overall highly robust deployment. While the development of a synchronous deployed system is no doubt challenging, the payoff is high, and the potential applications are widespread.

A. Background

A wide variety of large deployable subsystems have been demonstrated on spacecraft over the years. An early example from the late 1970s and 1980s is the Wrap-Rib[1] antenna that utilized a series of deployable ribs to support a large mesh antenna. Other significant milestones in lightweight, deployable space structures include the echo balloon series from the 1960s, the flexible solar array (FRUSA)[2] flown in 1971, the L'Garde inflatable decoys from

[1] Engineer, 1451 Innovation Parkway SE Suite 100, AIAA Member.
[2] Research Aerospace Engineer, Space Vehicles Directorate, 3550 Aberdeen Avenue SE, AIAA Senior Member.

Report Documentation Page

Form Approved
OMB No. 0704-0188

1. REPORT DATE	2. REPORT TYPE	3. DATES COVERED
APR 2007		**00-00-2007 to 00-00-2007**

4. TITLE AND SUBTITLE	5a. CONTRACT NUMBER
Synchronous Deployed Solar Sail Subsystem Design Concept	5b. GRANT NUMBER
	5c. PROGRAM ELEMENT NUMBER
6. AUTHOR(S)	5d. PROJECT NUMBER
	5e. TASK NUMBER
	5f. WORK UNIT NUMBER
7. PERFORMING ORGANIZATION NAME(S) AND ADDRESS(ES) **Air Force Research Laboratory,Space Vehicles Directorate,3550 Aberdeen Avenue SE,Albuquerque,NM,87117**	8. PERFORMING ORGANIZATION REPORT NUMBER
9. SPONSORING/MONITORING AGENCY NAME(S) AND ADDRESS(ES)	10. SPONSOR/MONITOR'S ACRONYM(S)
	11. SPONSOR/MONITOR'S REPORT NUMBER(S)

12. DISTRIBUTION/AVAILABILITY STATEMENT
Approved for public release; distribution unlimited

13. SUPPLEMENTARY NOTES
48th AIAA/ASME/ASCE/AHS/ASC Structures, Structural Dynamics, and Materials Conference, 23 - 26 April 2007, Honolulu, Hawaii

14. ABSTRACT

15. SUBJECT TERMS

16. SECURITY CLASSIFICATION OF:			17. LIMITATION OF ABSTRACT	18. NUMBER OF PAGES	19a. NAME OF RESPONSIBLE PERSON
a. REPORT **unclassified**	b. ABSTRACT **unclassified**	c. THIS PAGE **unclassified**	**Same as Report (SAR)**	**13**	

the 1970s and 1980s, and the L'Garde inflatable antenna experiment from the 1990s[3]. Deployable mast structures have also been used extensively over the years. Some of the most reliable have proven to be tubular booms and coilable masts[4]. It is anticipated that as spacecraft continue to be developed with an increasingly diverse level of functionality, the demand for novel deployable architectures will increase.

Solar sails are an exclusive class of large deployable space structures. Typical solar sail systems must rely heavily on tension-only members in order to maximize mass efficiency. For example, many baseline concepts consist of a highly flexible membrane film suspended between cables.[5,6,7,8] The structural compliance of these tension-only components renders them difficult to deterministically manage during deployment. For example these members must be continually tensioned throughout deployment in order to achieve predictable kinematic behavior. In the work herein these and other related challenges are identified and addressed through practical solutions.

B. Concept Overview

Figure 1 illustrates the baseline synchronous deployed solar sail concept with dimensions that reflect a ground demonstration unit. Upon first glance, one may notice a few of the unique physical features of this concept. For example a large inner opening is included in the film and a small opening is incorporated in the central hub structure. Edge length and inner diameter of the film are somewhat arbitrary and can be easily scaled to meet specific mission requirements. Structural architecture of the concept is detailed in the following list:

1. Central hub structure houses mast deployment mechanism, drum, stowed sail, and stowed masts
2. Four extendible masts attach to the central drum at discrete tangency points,
3. Inner and outer spar networks fasten to the four masts,
4. Series of radial tension cords link the inner and outer spar networks, and
5. Continuous membrane sheet is secured to each radial cord.

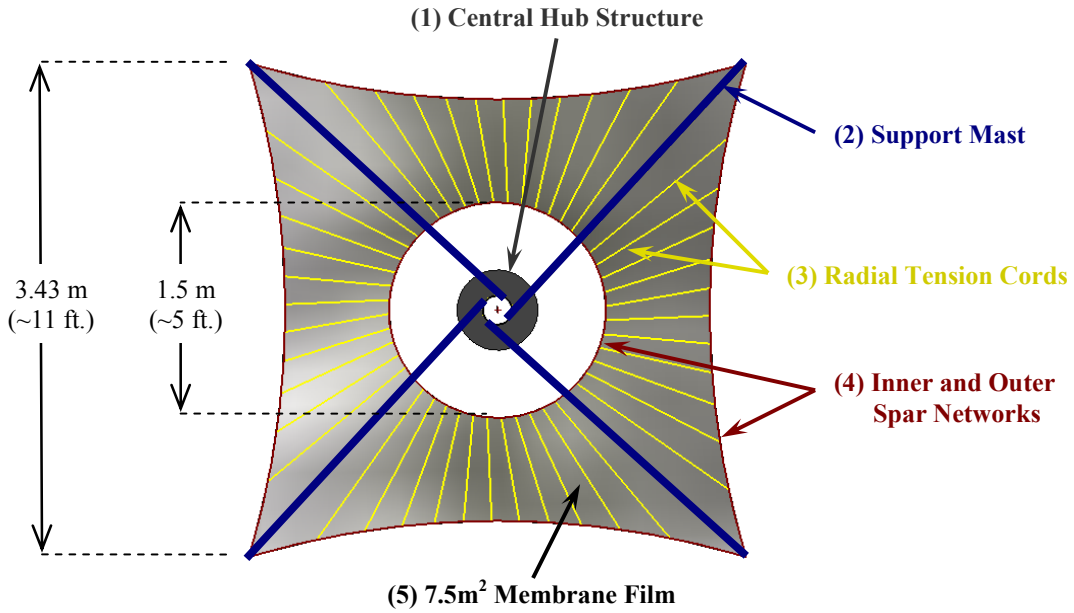

Figure 1. Synchronous deployed solar sail subsystem design concept.

Deployment is actuated by rotating the central drum to which the four masts are anchored. This rotation extends the masts along a tangency path to the drum stretching the spring-like inner and outer spar networks fastened to the masts. As these spar networks are stretched, they constantly pull against each other through a series of radial tension cords that serve to manage unfolding of the membrane film. While in the packaged state the film rests in a spiral wrapped configuration around the drum alongside the unstrained spars.

The inner and outer spars are critical to a well behaved deployment as they are tasked with constantly maintaining tension in the radial cords. This is accomplished due to the unique geometry of the spar network that emulates the corrugated pattern of the spiral wrapped surface. This geometry allows the spars to be relaxed while stowed and highly strained while fully deployed.

The membrane film is attached to the tensioned radial cords in such a way as to be "slack" throughout deployment. This feature is enabled by the fact that the spars follow the nominal kinematic path of the spiral surface

and the radial cords maintain tension throughout deployment. The membrane can then be relieved from the burden of assuring nominal kinematics—a task better left to more structurally equipped components such as masts and spars. The underlying assertion that the membrane film is merely "along for the ride" also simplifies the design/analysis process on first order by allowing the membrane to be decoupled from the support structure.

Figure 2 illustrates the deployment sequence of this concept. Notice that the sail and masts are simultaneously deployed allowing for a simple actuation mechanism and enabling short deployment times. This figure shows the nominal kinematic path. It is important for the sail to follow this nominal path as closely as possible to ensure proper tension is maintained in the radial cords which is a key to a reliable deployment. One of the challenges to achieving this well behaved kinematic behavior is to do so without the use of mechanical joints that would render the solar sail inefficient as a propulsion source due to high mass and poor packaging efficiency. Therefore the premise guiding this design is that the primary structure be erected from fully elastic members that require no assistance from mechanical joints to naturally follow the nominal kinematic path.

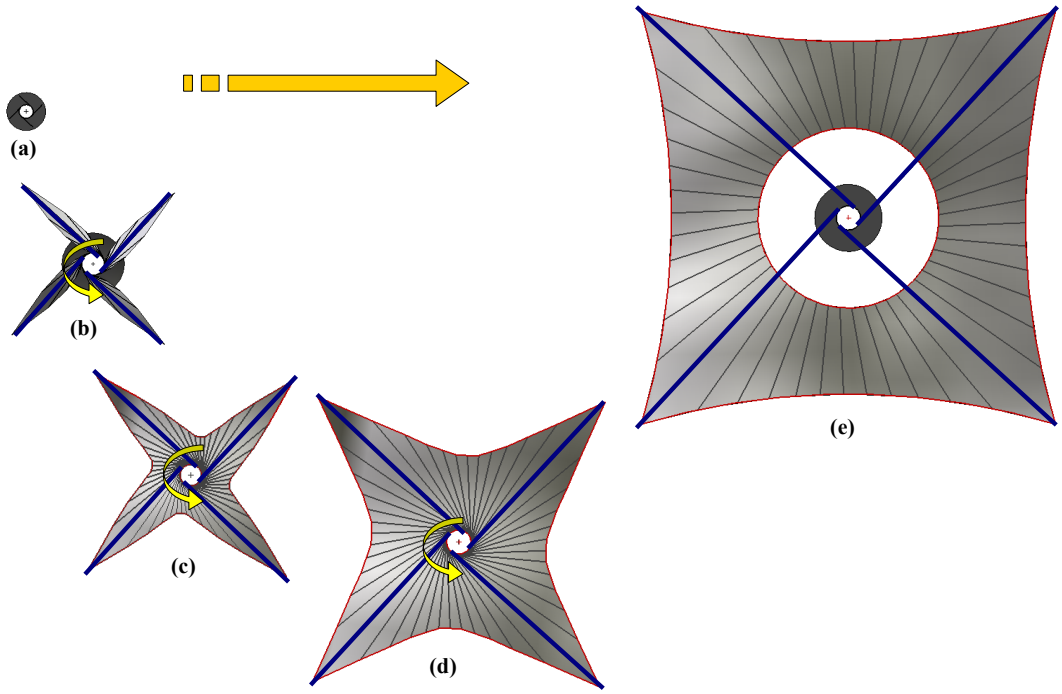

Figure 2. Masts and sail simultaneously deploy as shown for several instants during deployment: (a) stowed, (b) 40% deployed, (c) 55% deployed, (d) 70% deployed, and (e) fully deployed.

II. Surface Kinematics

Geometry of the solar sail concept originates from the spiral wrapped surface fold pattern defined in the early 1960's by Huso[9] and Lanford[10] as an automobile tarpaulin cover. Figure 3 illustrates how this surface allows a flat sheet to be wrapped around a drum with controlled and repeatable folding kinematics. In the 1990's, Guest[11] and Pellegrino characterized kinematics of this surface including a variation that accounts for thickness of the sheet. In addition, Shulz[12] defined the equilibrium deployment path of a rigid spiral wrapped surface for use as a reflector.

Several features of this folding pattern make it an ideal baseline for a synchronous deployed solar sail. First, the entire surface can easily be deployed by simultaneously pulling on only four discrete outer corners or by rotating the central drum counter clockwise. Both are evident in Fig. 3. Second, deployment path of these four points accommodates the use of many common collapsible, extendible, stiff members such as a Storable Tubular Extendible Member (STEM)[13], a lenticular tube[14] , or a tape-spring. Fig. 3d shows that the deployment path of this class of mast is identical to that of the spiral surface. The third benefit to this fold pattern is that it allows strain free attachment of the spiral surface to the mast. Therefore, deployment of the entire sail subsystem requires only that the masts be deployed. Furthermore, it is possible for one actuator to deploy all four masts and the main sail simultaneously. The fourth feature is that the z-fold configuration never allows a fold to double over onto another,

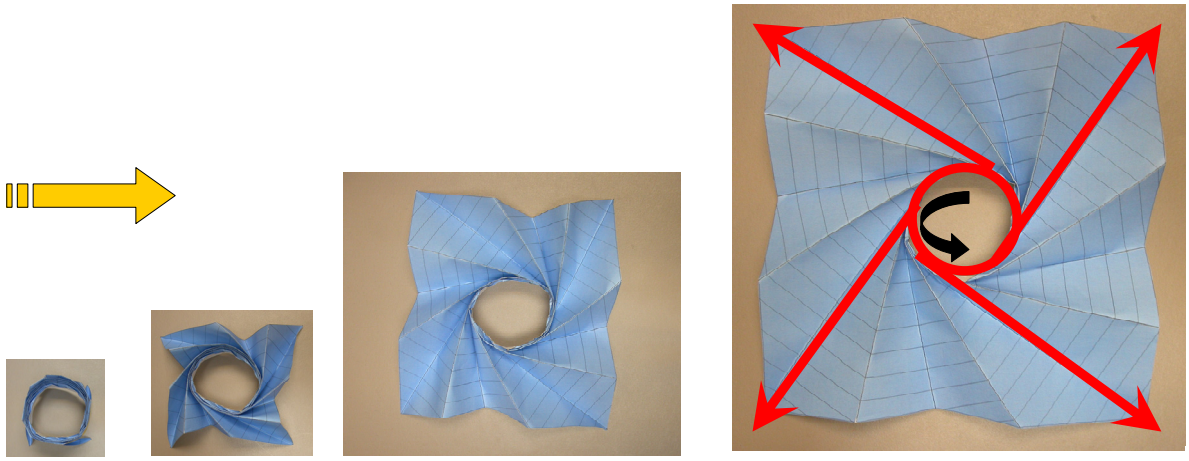

(a) **(b)** **(c)** **(d)**

Figure 3. Deployment sequence of the spiral wrapped surface is demonstrated on medium quality paper: (a) fully wrapped, (b) partially deployed, (c) mostly deployed, and (d) fully deployed. Notice that deployment path of the booms (red) emulates that of the surface (blue).

minimizing kinematic complexity and reducing the risk of entanglement. Based on these four features, the spiral wrapped surface was selected as the baseline folding pattern for this synchronous deployed solar sail concept.

The baseline spiral wrapped surface fold pattern was slightly modified to ensure the deployment path of each "valley" fold (see Fig. 4) tracks along one common planar kinematic path. The purpose of this modification is for the sake of mechanism simplicity in that each of the four masts are able to track co-planar to each other rather than on a slightly downward angle. This modification also has the added benefit that the masts stack up uniformly onto the drum while stowed. Notice from Fig. 4 that the valley folds on the original spiral surface track along a helix during deployment, but on the modified spiral surface they track along a single plane.

This modified feature was realized by shifting each "peak" fold toward the clockwise neighboring valley fold by a distance defined by Eqn. 1 as referenced to Fig. 5.

$$w = \frac{L}{2\cos\left(\frac{\pi-\alpha}{2}\right)\tan\left(\alpha-\frac{\pi}{2}\right)} \tag{1}$$

And α is defined by Eqn. 2.

$$\alpha = \left(1-\frac{2}{n}\right)\pi \tag{2}$$

And Eqn. 3 defines the length of one side of the polygonal drum.

$$L = \frac{R\sin\left(\frac{2\pi}{n}\right)}{\sin\left(\frac{\alpha}{2}\right)} \tag{3}$$

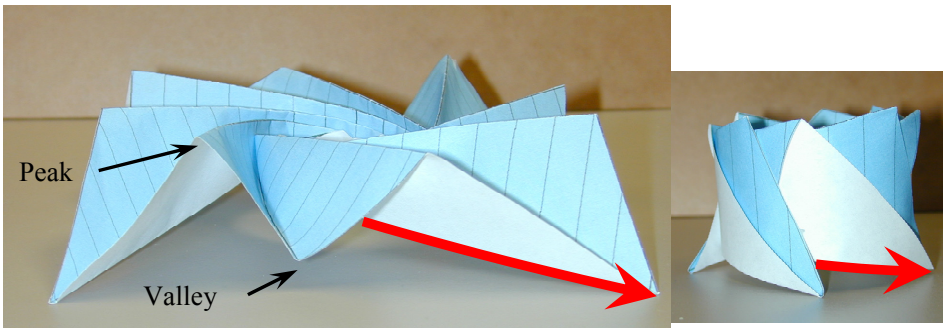

(a)

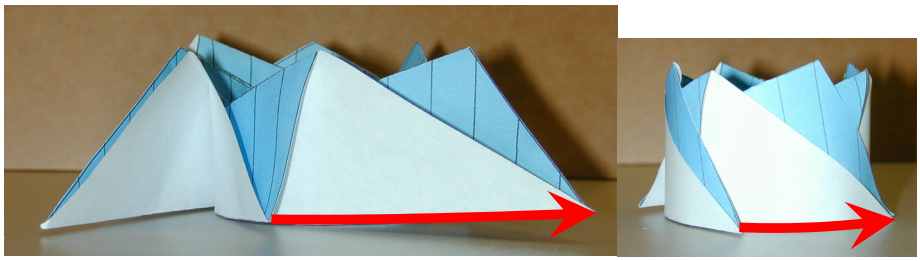

(b)

Figure 4. Peak and valley folds both form a helix on the original spiral surface (a) causing an undesirable downward mast deployment path (red arrow), but valley folds lie flat for the modified spiral surface (b) enabling the masts to deploy horizontally.

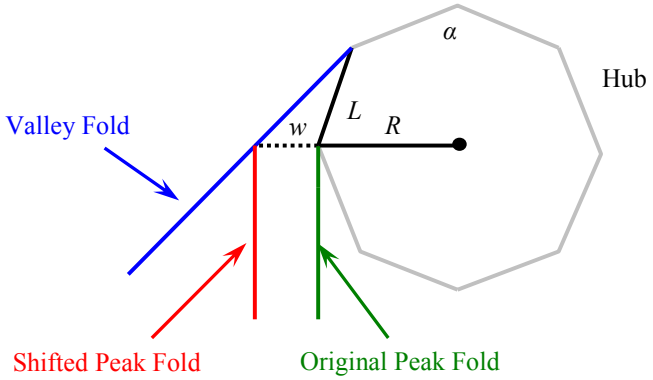

Figure 5. Spiral wrapped surface was modified by shifting all peak folds by w. This introduces a small kinematic irregularity of distance s.

After this modification the area near the apex of each radial fold becomes kinematically problematic because the shifted valley folds no longer apex at the central drum. For this reason, the center cutout area is expanded and the number of polygon sides is reduced from n to n/2. Figure 6 shows how the fold lines of the modified spiral surface differ from the original. Notice that the peak folds are shifted in Fig. 6b and the center cutout area is expanded in Fig. 6c.

It is worthy to note that kinematic irregularity is immediately introduced into the surface after deployment begins in the form of a small shear strain between each pair of peak and valley folds. Certainly one of the goals of this solar sail is to achieve a perfect kinematic path to ensure a smooth and uneventful deployment. In practicality however a small amount of elastic shear deformation between peak and valley folds must be acceptable. The thin membrane sheet draped between the adjacent peak and valley tension cords should provide adequate shear compliance to relieve this small shear stress without becoming a significant load path.

Another modification to the spiral wrapped surface was also considered. Until now the fold pattern has neglected any effects due to thickness of the wrapped sail. In reality the film and spars have some finite thickness, but it turns out that in practice this thickness has a negligible effect on sail folding. Pellegrino[4] presents a

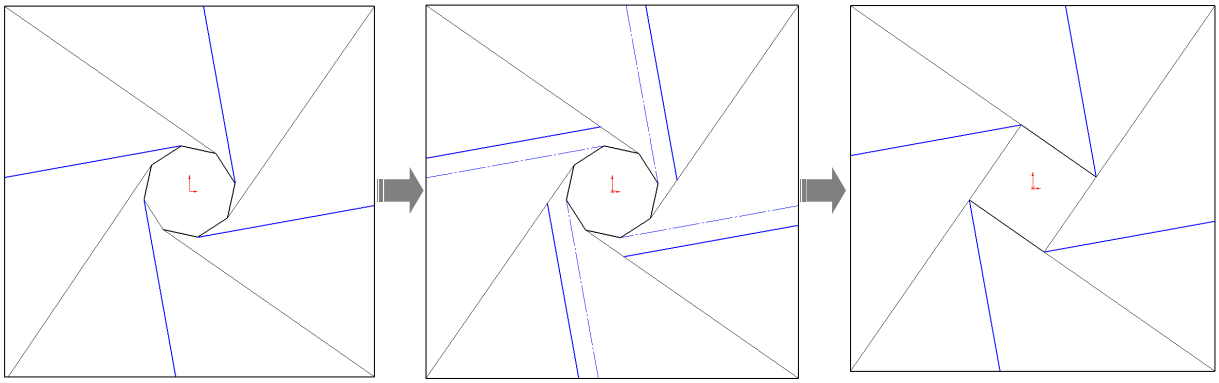

(a) (b) (c)

Figure 6. Progression of changes to the fold pattern: (a) original, (b) peak folds shifted toward valley folds, and (c) cutout enlarged and reduced to n/2 sides to form the modified fold pattern.

straightforward methodology to accounting for this thickness on the original spiral wrapped surface. A single radial fold line is approximated as a series of short straight cords connected at slightly increasing angles (never more than 180º) such that in the deployed configuration, these radial fold lines form a slight spiral rather than a straight line. And in the deployed configuration, these fold lines form a spiral of slightly increasing radius rather than a spiral of constant radius. This method successfully achieves perfect kinematic regularity—clearly an essential goal when dealing with gores of rigid plates. But the current structure of interest uses highly shear compliant membrane gores. The kinematic effects of neglecting wrap thickness are secondary for this thin architecture e.g., a slight shear strain between neighboring peak and valley folds. Accounting for wrap thickness would present significant manufacturing complexities particularly for the masts because they would need to possess a natural eccentricity of slightly increasing radius to emulate the curved radial fold lines.

The selected number of gores in this solar sail concept is an important design facet that dictates the wrapped sail height. Equation 4 expresses the relationship between the stowed height, the number of gores, and the characteristic length of one side of the square sail.

$$h = \frac{2\pi\left(\frac{s^2}{2}\right)^{1/2}}{n} \tag{4}$$

Clearly the stowed height decreases directly as the number of gores increases. As the number of gores is increased the wrapped thickness also increases. Using the variables in Eqn. 4 sail geometry can be tailored to meet specific packaging requirements. However increasing the number of gores adds mass to the system and should be carefully considered when selecting the number of gores for a specific sail mission.

An additional modification can be implemented on the spiral surface that greatly increases the packaging efficiency. It was discovered that back folding each peak fold into a secondary fold can drastically reduce the wrapped sail height without the added wrap thickness of increasing the number of gores as demonstrated in Fig. 7. Secondary folds can reduce the wrapped sail height by a factor of two if their apex is positioned at the peak fold line half-length as shown in Fig. 8. The downside to using secondary folds is that the spar structure needed to guide these folds along the correct kinematic path adds significant complexity to the subsystem unless an elegant solution can be realized. In practice, priority of specific spacecraft requirements (e.g., packaged volume, mass, geometry, and risk acceptability) will dictate the prudent use of secondary folds on a solar sail subsystem.

The secondary folding pattern presented in Fig. 8 resembles the "rotationally skew fold" pattern proposed by Furuya[15] for a spinning deployed solar sail. His pattern is a recursive application of the secondary fold proposed here, albeit with a much different deployment strategy.

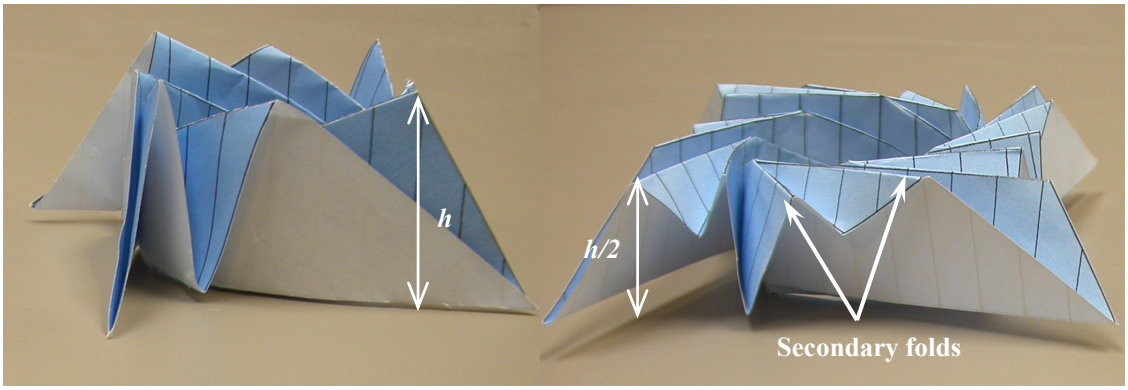

(a) (b)

Figure 7. The modified spiral wrapped surface is shown without (a) and with (b) secondary folds to show the reduced stowed height from h to h/2.

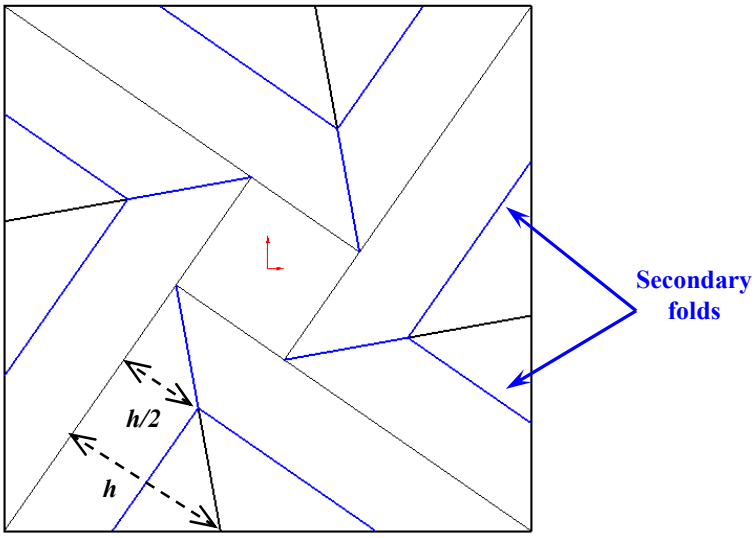

Figure 8. Secondary folds can reduce the wrapped height, h, by a factor of two if the apex is positioned at the peak fold half-length as shown. (Blue indicates a peak fold and black a valley fold.)

III. Elastic Behavior

Unlike many deployable planar structures, this concept avoids reliance on mechanical joints to enforce proper kinematics. Unfolding is controlled by two networks of spring-like spar members that must continually emulate the nominal spiral surface geometry during deployment. The radial cords suspended between the spar networks must then be continually tensioned to ensure the film is managed properly and to ensure the structure is elastically stable.

In addition to these two critical functions, the spars must perform according to the following metrics:

1) Low mass,
2) High stiffness,
3) High strain to failure for good deployed flatness,
4) Low reaction loads imparted to the support masts,
5) Reasonable manufacturability,
6) Low stowed height,
7) Able to accommodate radial cord attachment, and
8) Smooth edges to ensure the adjacent membrane film is not damaged.

Figure 9 shows several inner spar (IS) concepts, all composed of a resilient material. Each of these concepts represents one quadrant of the total inner spar network. The two lower tabs on the concepts indicate where the

masts attach. Geometry of each concept is a variation on the baseline geometry that consists of the peak and valley node locations along the inner spiral surface edge. Any conceivable geometry that connects these nodes could emulate proper kinematics. However the elastic behavior of such geometry must be considered with respect to the previously listed spar design criteria.

Deployment of each concept in Fig. 9 was simulated using the ABAQUS/Standard[16] finite element code. Each spar was observed for material failure, radial cord tensions, and reaction loads at the mast attachment tabs. As mentioned previously, proper radial cord tension is critical to this sail design. However material strength and mast loading were the primary metrics of interest at this point because accurate radial cord tension predictions are only possible when modeling the coupled interaction between the inner and outer spars.

Several conclusions were deduced from the inner spar deployment analysis. First, the maximum deployed flatness is achieved when the node regions are curved to the maximum possible radius. Second, spar deformation emulates nominal kinematics best the node regions are symmetric about the peak and valley nodes shown in Figs. 9d through 9h. Notice from the figure that the peak node regions are angled downward by 7.5˚ and the valley regions lie horizontal. (This 7.5˚ angle is determined by dividing 360˚ by the number of gores, 48.) Third, the radial cord tensions are influenced by the non-linear bending stiffness of the two adjacent inner spar legs, i.e., the spar becomes stiffer the further it is stretched and the cords gain more tension as a result. This non-linear behavior is unavoidable for this spiral geometry, but it can be minimized by utilizing the bending stiffness of the spar legs as much as possible and avoiding any twist deformations that tend to drastically reduce stiffness. The geometry that produced the most linear stiffness is a straight spar leg connecting adjacent peak and valley nodes; however, a straight spar leg makes for poor strength performance because it causes high stress concentration near the node regions. Therefore, a compromise was reached in which the node regions are curved somewhat and the leg regions between them are nearly straight as shown in Figs. 9f, 9g, and 9h.

It should be noted that inner spar geometry prevents the sail from ever deploying to a completely flat configuration. For example, the inner spar is relaxed and strain free in the stowed state and is strained the most in the fully deployed state and unable to flatten. Thus sail topology remains slightly corrugated at full deployment. Actual deployed flatness of the sail is dictated by material strength limits of the inner spar.

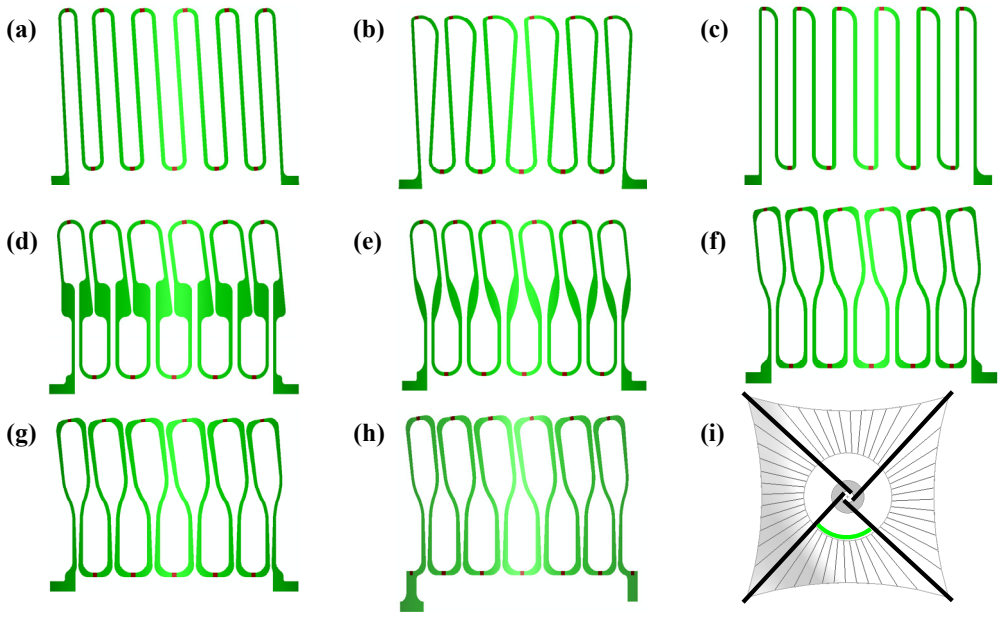

Figure 9. Several different inner spar concepts were formulated and analyzed: (a) IS1, (b) IS2, (c) IS3, (d) IS4, (e) IS5, (f) IS6, (g) IS7a, and (h) IS7b. Each represents one sail quadrant shown with respect to full-system (i).

Several outer spar (OS) concepts were developed under the same basic premise as the inner spar concepts. In fact many of the lessons learned from the inner spars were applied to the outer spars. For example, node regions were initially sized to a large radius of curvature to prevent high stress concentration areas while keeping the legs between them of reasonable straightness in order to avoid any severe non-linear stiffness effects from excessive twist deformations.

It is not possible to accurately evaluate outer spar elastic behavior without including the coupled interaction of the inner spar and radial cords. Therefore a structural model was created to simulate deployment of one stowed sail quadrant using the ABAQUS/Standard finite element code. Figure 10b shows the finite element model (FEM) geometry including the outer spar (OS1ba and OS1bb), inner spar (IS7b), radial cords, and a central drum. The membrane film was not included in this model due to the previously stated assumption that the film is not a significant load carrying component as long as nominal kinematics is upheld. Shell elements are used to represent the inner and outer spar plates, truss elements represent the radial cords, and an analytical rigid body is used to simulate the central drum. Contact was defined between the rigid drum and the structural elements to ensure the sail deployment path includes a trip around the drum. For the sake of simplicity, the masts are replaced with displacement controlled boundary conditions at the lower spar tabs. These boundary conditions model the nominal deployment path of two masts. Notice from Fig. 10b that the spars are not wrapped around the drum in the stowed state. Instead they lie in a single plane and are translated along that plane until each of the four tabs reach the drum. Once they reach the drum the tabs are translated along the true mast deployment path tangent to the hub. This modeling technique greatly increases computational efficiency while accurately representing the elastic behavior of the main sail during deployment.

The seemingly random geometry of the sail support structure in Fig. 10b was derived from a two-dimensional drawing of the modified spiral fold pattern. One quadrant of this fold pattern is shown on left-hand side of Fig. 10a. Wrapped sail geometry was realized by pivoting the two masts toward each other while folding each gore between them in a corrugated z-fold fashion similar to way a Victorian fan is folded. Each node in the drawing is treated as a one degree of freedom pivot. Notice from the figure that the inner spar is colored green, outer spar A is colored blue, and outer spar B is colored red. This collapsed geometry then generates the critical peak and valley node locations used for reference to create the exotic spar shapes shown in Fig. 10b as well as to determine radial cord lengths.

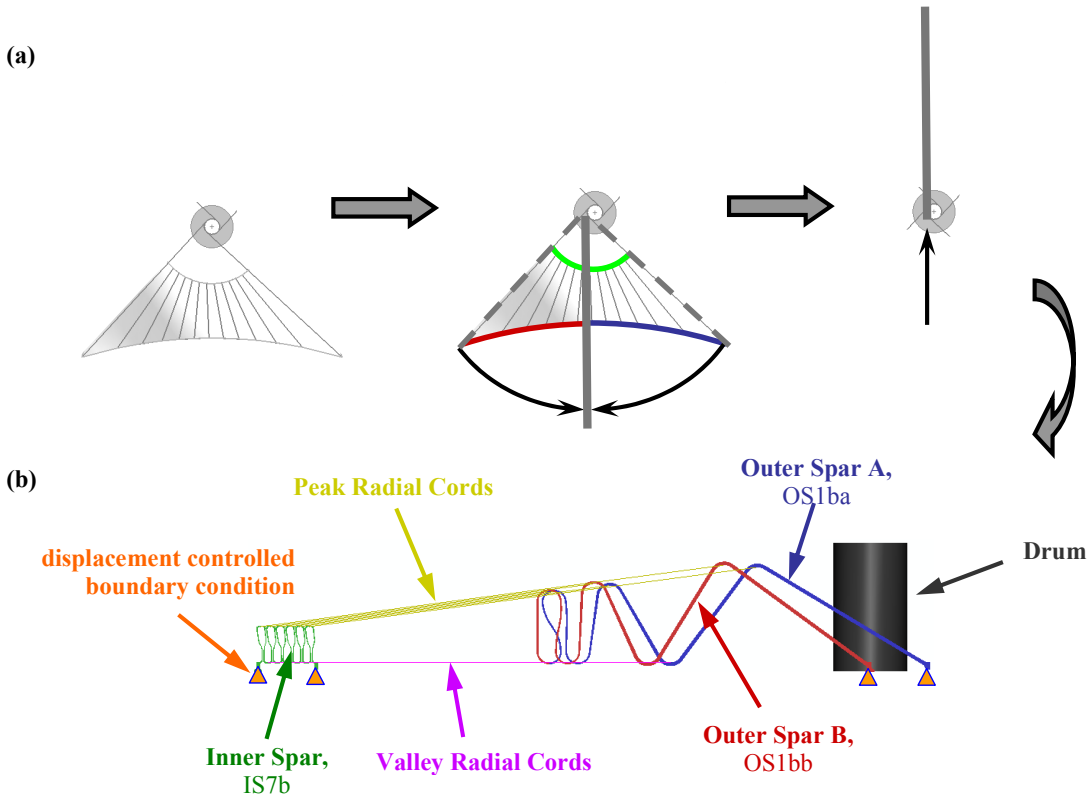

Figure 10. Geometry of one sail quadrant was determined by collapsing each component into a single plane (a). A finite element model (b) of this geometry was created to predict behavior of the sail during deployment.

Several key insights were deducted from deployment simulations of the four different outer spar concepts shown in Fig. 11. First, nominal kinematic behavior is only achieved when the outer spar stiffness and the inner spar stiffness are balanced. If the outer spar is too stiff then the inner spar will be stretched beyond the nominal kinematic path, and this would cause the membrane film to endure shear strains. Similarly, if the outer spar is too compliant then it will be stretched beyond the nominal kinematic path by the inner spar with the same detrimental effect on the membrane film. In fact the distance that the spars stray from the nominal path can be directly correlated to the level of shear stress imparted on the membrane film. As has been previously stated, any significant shear loads that may force the film to become a primary load path must be avoided.

A second insight deduced from this one-quadrant analysis is that once nominal kinematic behavior is achieved, radial cord tensions tend to become relatively uniform. This insight is vitally important to the reliability of this system. Continuously positive and relatively uniform radial cord tensions indicate a stable, well behaved structure. Any local low stiffness points at any instant or any global low stiffness events indicate a possible elastic instability that may cause the sail to fold non-deterministically. However it is important to note that the spiral fold pattern in use here prevents the radial cord tensions from ever becoming perfectly uniform either among all cords during any one instant or at one cord during all instants of deployment. Therefore in practicality, the goal is not perfectly uniform cord tensions but rather relatively uniform cord tensions.

Figure 11 shows a plan view of the predicted deployed shape overlaid onto the nominal deployed shape for each of the four outer spar concepts. Notice that OS1a shown in Fig. 11a is much too compliant especially near the outer edges where the nodes have displaced inward from the nominal position. This may be the result of the highly compliant, long, thin, sweeping curvature of the outer leg geometry inherent to the OS1a concept. This observation leads to the conclusion that outer spar stiffness may need to be tuned locally at each individual spar leg and node region in addition to being tuned globally.

Tuning spar stiffness requires simultaneous adjustment of several dimensions including width and curvature node regions and width of the legs. Each dimension must be carefully considered with respect to the span of the respective leg in question. Notice in Fig. 11b that the outer legs (right-hand side of the spar) on OS1b are thicker than the interior legs (left-hand side of the spar). The reason for this inconsistent width is to help balance the stiffness of the longer spans with respect to the shorter spans. For OS1b the stiffness was further adjusted by downsizing the radius of each node region to one consistent value. While any radius is permissible, a smaller radius is advisable because it allows the spar legs to be straighter which prevents excessive spar leg twisting during deployment, a behavior that has been shown to cause highly nonlinear radial cord tensioning. After increasing stiffness by increasing the leg width and by decreasing the node region radius, OS1b strain levels were checked at full deployment to ensure they remained below any material strength limits. Comparing the predicted deployed shapes for OS1a and OS1b clearly indicates that the geometric adjustments are indeed helpful in achieving nominal kinematic behavior; OS1b emulates the nominal shape much better than OS1a. And it is anticipated that further stiffness tuning will enable an even better kinematic performance.

Another parameter that may be adjusted to help balance tension between the inner and outer spars is the outer scallop shape. Figure 11a and 11b show the baseline outer scallop shape which is a constant radius about four times greater than the inner scallop radius. Other variations include a straight outer scallop as shown in Fig. 11c or an irregular scallop shape as shown in Fig. 11d. As one might expect, the straight outer scallop produced poor kinematic behavior as the predicted shape deviated significantly from nominal.

The irregular shape in Fig. 11d was surprisingly unsuccessful at achieving nominal kinematics as well. This concept was created by giving the outer scallop a constant radius in the partially wrapped geometry rather than in the fully deployed geometry. The purpose was to achieve uniform cord tensions in the partially wrapped state particularly at the point when the inner spar leaves the drum. The predicted shape for this concept in Fig. 11d shows that designing the scallop shape around a partially deployed configuration is not a prudent design approach.

It turns out that the scallop shape that enables the best kinematic performance (and most uniform radial cord tensions) is a constant radius like that incorporated on OS1a and OS1b in Figs. 11a and 11b respectively. Optimum scallop depth is directly related to the global inner and outer spar stiffness balance. For example, the shallower the outer scallop, the greater the outer spar stiffness required to properly counter-load the inner spar. In fact, the outer scallop depth and outer spar geometry selected for the baseline OS1b in Fig. 11b is shown to be of reasonable stiffness to properly counter-load the inner spar. Therefore a good rule of thumb is an outer scallop radius that is four times that of the inner scallop. However this rule may not apply for sail sizes different than this 7.5 m^2 concept. In fact for some missions it may be prudent to sacrifice sail deployed flatness for an increase in deployed area. For example increasing outer spar global stiffness causes higher spar strain levels that reduce the deployed flatness but allow the outer scallop depth to be decreased producing more sail area.

The selected baseline system configuration is shown in Fig. 11b. The IS7b inner spar and the OS1b outer spar combination exhibit reasonable kinematic regularity and properly tensioned radial cords throughout deployment. Figure 12 shows the predicted shape of this concept at two stages during deployment. Figure 12a shows the shape at 70% deployment when the inner spar leaves the drum, and Fig. 12b shows the predicted shape at 95% deployment when the spar material reaches the material strain limit. Upon reaching this limit, the total projected sail area is 7.0 m^2, 92% of the 7.5 m^2 actual membrane area. As this architecture is scaled up, the deployed area efficiency is expected to improve.

As has been exhaustively discussed, this sail concept must achieve nearly nominal kinematic behavior during deployment to ensure reliability and elastic stability. Achieving this metric is largely dictated by proper inner and outer spar stiffness and by a proper outer scallop shape. Three specific spar dimensions must be adjusted together to achieve proper local and global spar stiffness: leg width, node region width, and node region radius. Outer scallop depth must be carefully selected with respect to the global outer spar stiffness. A well behaved structure is achievable when these parameters are properly adjusted according to previous discussions.

While the baseline synchronous deployed solar sail concept performs well, it is anticipated that performance can be enhanced by further tuning the spar stiffness and by adjusting the outer scallop depth. A full-scale ground demonstration of this concept is the next step in determining how much additional tuning is required to ensure a stable and reliable deployment.

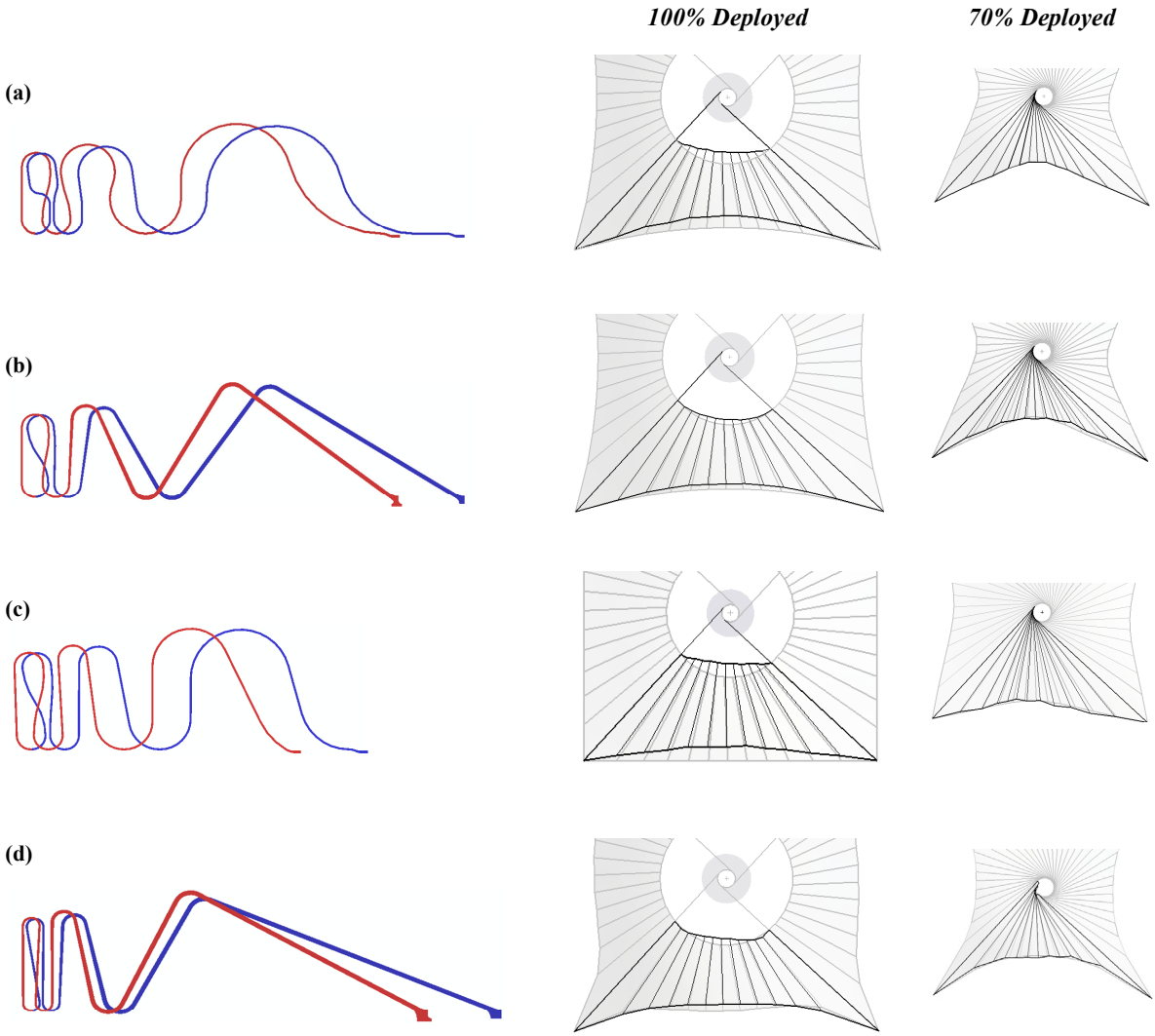

Figure 11. Four different outer spar concepts were evaluated for their ability to emulate the nominal kinematic shape. (a) OS1a, (b) OS1b, (c) OS2, and (d) OS3 are shown in the stowed form, the nominal kinematic shape (gray), and the predicted shape (black) at two different instants during deployment.

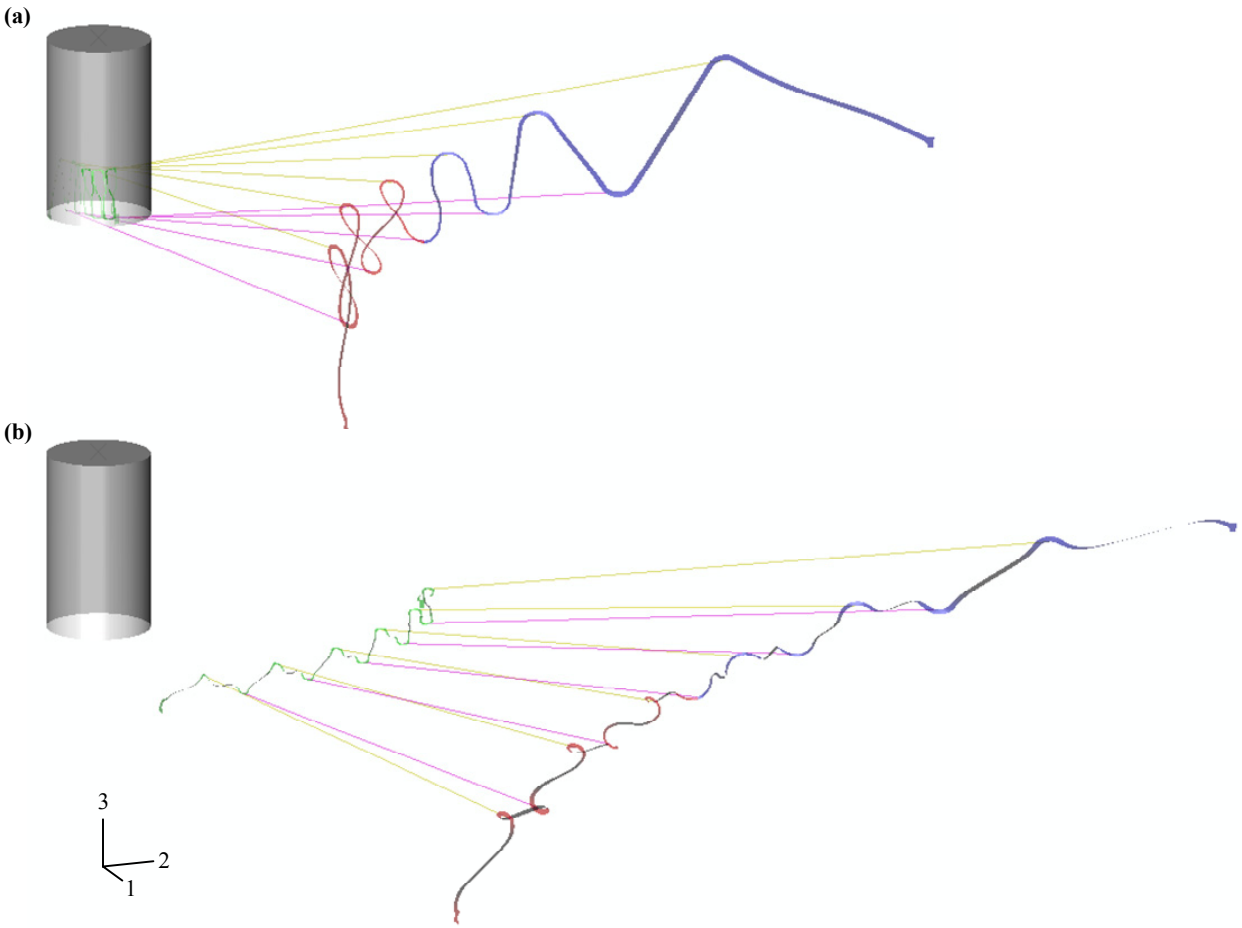

Figure 12. One quadrant of the solar sail is shown at (a) 70% deployed and at (b) 95% deployed when the spar material reaches the strain limit as predicted by the FEM.

IV. Summary

As the spacecraft community continues to rely upon large deployable structures to fulfill new mission requirements, new architectures must be developed. The novel solar sail concept presented in this study offers a simple and robust deployment method that enables the support structure to be constructed of a single material, free from any mechanical joints. The only actuation necessary is the rotation of a central drum to which four rollable extendible masts are anchored. These masts are attached to a series of spring-like spar members that tension a set of radial cords used to manage film unfolding. Spar members are a key to this design in that they provide continuous tension in the cords throughout deployment. And continuous tension is a prerequisite to achieving elastic stability and deterministic unfolding, both of which are realized in this design. While this membrane structure was originally intended as a propulsion medium, the simple, robust features of this subsystem may prove valuable to reducing mass and increasing deployment reliability of other deployable planar subsystems such as sun shades, solar arrays, radiators, or antenna arrays.

Acknowledgments

Support of this work is sponsored by the Air Force Research Laboratory Space Vehicles Directorate monitored by Dr. Jeffry Welsh.

References

[1] Wada, B. K., Freeland, R. E., Woods, A. A., "Development of the Structural Technology of a Large Deployable Antenna," 13th International Symposium on Space Technology and Science, Proceedings, Tokyo, Japan, June 28-July 3, 1982, pp. 395-400.

[2] Olson, M., "Flexible Solar-Array Mechanism," Proceedings of the 7th Aerospace Mechanisms Symposium, NASA TMX-58103, Sept. 1972. pp. 233-249.

[3] Chielewski, A., "Overview of Gossamer Structures," Gossamer Spacecraft: Membrane Inflatable Structures Technology for Space Applications, Edited by C.H.M. Jenkins, Vol. 191, Progress in Astronautics and Aeronautics, AIAA, Virginia, 2001, pp. 1-33.

[4] Pelligrino, S., "Large Retractable Appendages in Spacecraft," Journal of Spacecraft and Rockets, Vol. 32, No. 6, November-December 1995.

[5] Forward Unlimited, "Gossamer Spacecraft Survey Study, Preliminary Report – Historical Survey," Jet Propulsion Laboratory, JPL Prime Contract NAS7-1407, July 18, 1999.

[6] Murphy, D., Murphey, T., Gierow, P., "Scalable Solar Sail Subsystem Design Concept," AIAA Journal of Spacecraft and Rockets, Vol. 40, No. 4, July-August, 2003.

[7] Lichodziejewski D., Derbes, B., West, J., Reinert, R., Belvin, K., Pappa, R., "Bringing an Effective Solar Sail Design Toward TRL 6," 39th AIAA Jet Propulsion Conference and Exhibit, AIAA 2003-4659, Huntsville, Alabama, July 20-23, 2003.

[8] Leipold, M., Garner, C.E., Freeland, R., Herrmann, A., Noca, M., Pagel, G., et al., "ODISSEE – A Proposal for Demonstration of a Solar Sail in Earth Orbit," European Conference on Spacecraft Structures, Materials and Mechanical Testing, Proceedings, Braunschweig, Germany, November 4-6, 1998, pp. 245-254.

[9] Huso, M. A., "Sheet Reel," U.S. Patent 2942794, 1960.

[10] Lanford, W.E., "Folding Apparatus," U.S. Patent 3010372, 1961.

[11] Guest, S., Pelligrino, S., Vincent, J., "Inextensional Wrapping of Flat Membranes," First International Seminar on Structural Morphology, Montpellier, 1992, pp. 203-215.

[12] Shulz, M., Pellegrino, S., "Equilibrium Paths of Mechanical Systems with Unilateral Constraints, II. Deployable Reflector," Proceedings of the Royal Society A: Mathematical, Physical, and Engineering Sciences, Volume 456, Number 2001 / September 8, 2000, pp. 2243-2262.

[13] Hazelton, C., Gall, K., Abrahamson, E., Denis, R., Lake, M., "Development of a Prototype Elastic Memory Composite STEM for Large Space Structures," 44th AIAA Structures, Structural Dynamics, and Materials Conference, 2003-1977, Norfolk, Virginia, 2003.

[14] Leipold, M., Runge, H., Sickinger, C., "Large SAR Membrane Antennas with Lightweight Deployable Booms," 28th ESA Antenna Workshop on Space Antenna Systems and Technologies, ESTEC, Noordwijk, 2005.

[15] Furuya, H., "Concept of Rotationally Skew Fold Membrane Spinning Solar Sail," 55th International Astronautical Congress of the International Astronautical Federation, the International Academy of Astronautics, and the International Institute of Space Law, IAC-04-I.1.05 Vancouver, Canada, Oct 4-8, 2004.

[16] ABAQUS/Standard User's Manual, version 6.6-3, Hibbitt, Karlsson, and Sorensen, Inc., 2006.